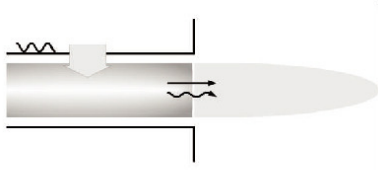Stephan Reuter (Autor)
Formation Mechanisms of Atomic Oxygen in an Atmospheric Pressure Plasma Jet Characterisied by Spectroscopic Methods

Stephan Reuter

Formation Mechanisms of Atomic Oxygen in an Atmospheric Pressure Plasma Jet Characterised by Spectroscopic Methods

Cuvillier Verlag Göttingen

https://cuvillier.de/de/shop/publications/1523

Chapter 3

The Atmospheric Pressure Plasma Jet (APPJ)

In this chapter, the atmospheric pressure plasma jet (APPJ) is presented. Following a description of the classical setup, consisting of two concentric electrodes, the modified planar APPJ, developed for this study, is introduced. The jet's working principle as well as characterising thermal, electrical, and spectroscopic measurements are presented, distinguishing its two substantial sections: discharge and effluent.

3.1 Setup of the APPJ

The atmospheric pressure plasma jet (APPJ) is a capacitively coupled radio frequency discharge usually operated at 13.56 MHz. The original setup of the APPJ, developed by Selwyn, Hicks, and coworkers [Selwyn99], was modified during the course of this study. In this chapter, a description of the classical (concentric) APPJ setup is followed by the presentation of the modified (planar) setup, developed to allow insight into the jet's glow discharge region.

3.1.1 Concentric APPJ

A schematic of the APPJ is shown in figure 3.1. The jet consists of two concentric stainless steel electrodes with an interjacent polytetrafluoroethylene (PTFE) spacer. The spacer aligns the inner electrode so that a uniform electrode gap along the entire electrode length is ensured. Furthermore, the PTFE-spacer insulates the outer electrode from the inner one, and it also functions as diffuser and stopper for the feed
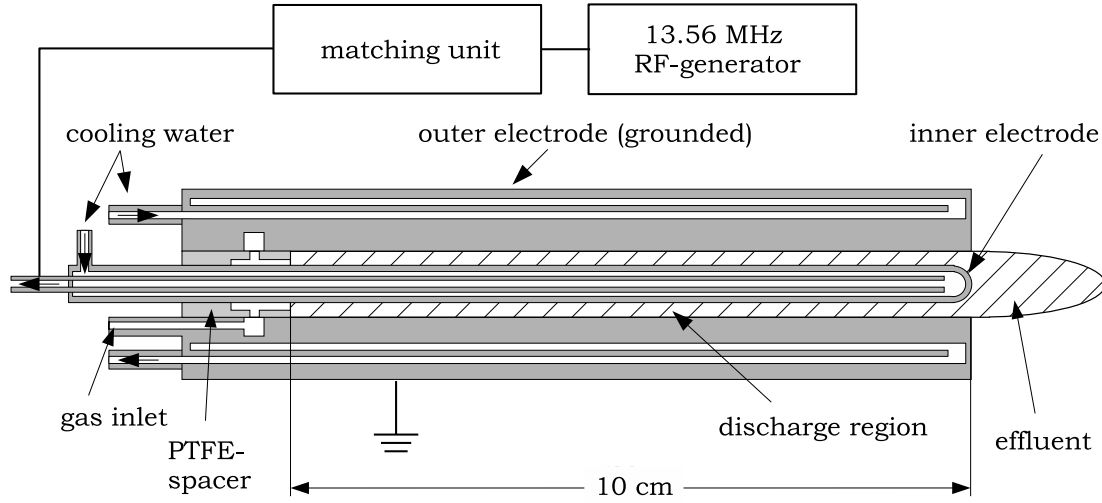
Figure 3.1: Schematic of the concentric APPJ

gas. The outer electrode's inner diameter measures 14 mm. Two exchangeable inner electrodes allow an electrode gap of 2 mm and 1.1 mm respectively. The effective electrode length is 10 cm. To ensure an even and smooth surface, the electrodes are electropolished. Each electrode is double-walled and water cooled, having a water in- and outlet at the rear side of the jet. The cooling water flux is $140 \, \mathrm{lh^{-1}}$. Inner and outer electrode have a parallel cooling circuit to inhibit parasitic resistances through the cooling water. The outer electrode is grounded while the inner electrode is connected to an L-type matching network and a 13.56 MHz RF-generator. The L-network prevents reflection of the RF-power by impedance matching of the dis-
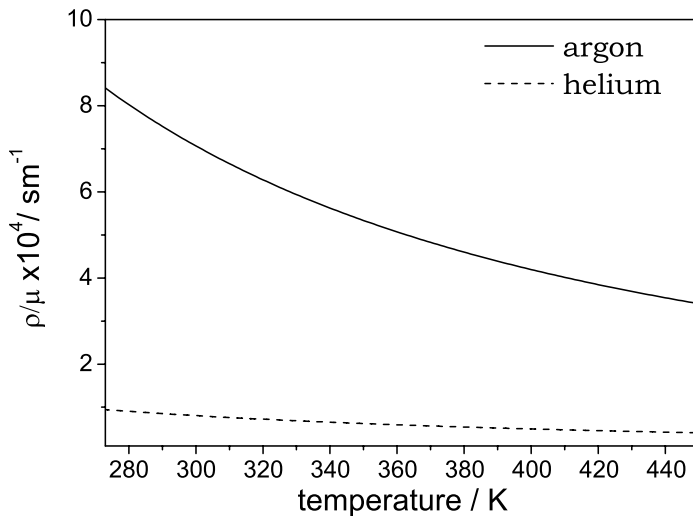

Figure 3.2: $q = \frac{\rho}{\mu}$ as a function of gas temperature (values for viscosities and densities are taken from [Lemmon05])

charge to the RF-generator [Norström79]. The jet can be operated at powers ranging from 20 to about 200 Watt. In the low power regime, the discharge runs unsteady or is not ignited, in the high power regime, the glow discharge constricts to an arclike- or γ-mode discharge [Yang05b, Wang03].

The electric, water, and gas connections of the jet are shielded by a brazen casing. The feed gas consists of 0.5 to 4 m³h⁻¹ noble gas (helium or argon with a purity of 99.999 %) with an admixture of oxygen in the order of 1 vol% (99.999 % purity), controlled by flowrators. A laminar gas flow can be assumed at these flow rates, since approximations of the Reynolds number for the setup and parameters used in this work are all below the critical Reynolds number of 2100 [Rott90]. The Reynolds number can be calculated by equation 3.1:

$$Re = \frac{d\rho\bar{v}}{\mu} = d\bar{v}q \tag{3.1}$$

with $q = \frac{\rho}{\mu}$, a dynamic viscosity for argon of $\mu_{Ar}(300 \text{ K}) = 2.2613 \cdot 10^{-5}$ Pa, a dynamic viscosity for helium of $\mu_{He}(300 \text{ K}) = 1.993 \cdot 10^{-5}$ Pa, an argon density of $\rho_{Ar} = 1.6025$ kg·m⁻³, and a helium density of $\rho_{He} = 0.1604$ kg·m⁻³ [Lemmon05, Macrossan03]. $\bar{v}$ is calculated from the gas flux in kg·m⁻³ and a cross sectional area of the jet of $A_{d=1.1 \text{ mm}} \approx 0.45$ cm² and $A_{d=2 \text{ mm}} \approx 0.75$ cm² respectively. Figure 3.2 shows that $Re \propto q$ decreases with gas temperature. In figure 3.3 the Reynolds numbers are plotted versus the gas flux for helium and argon at 300 K. Since the APPJ's gas temperature never subsides below 300 K, these are the maximal Reynolds numbers to be expected.
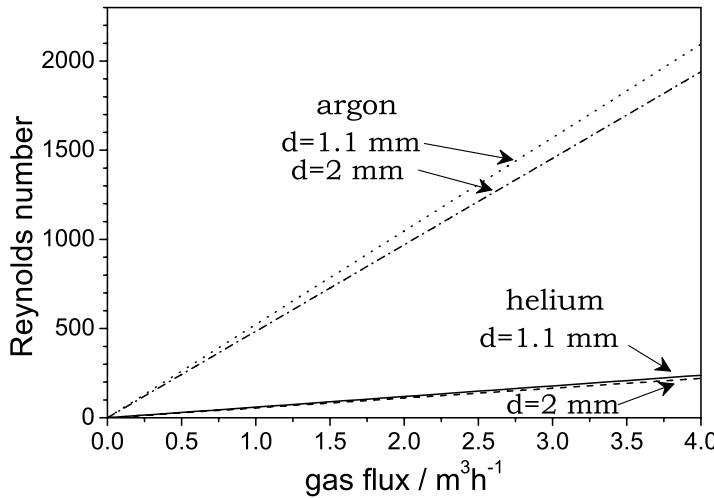

Figure 3.3: Reynolds number at 300 K for helium and argon base gas and for two different electrode gaps of 1.1 mm and 2 mm respectively
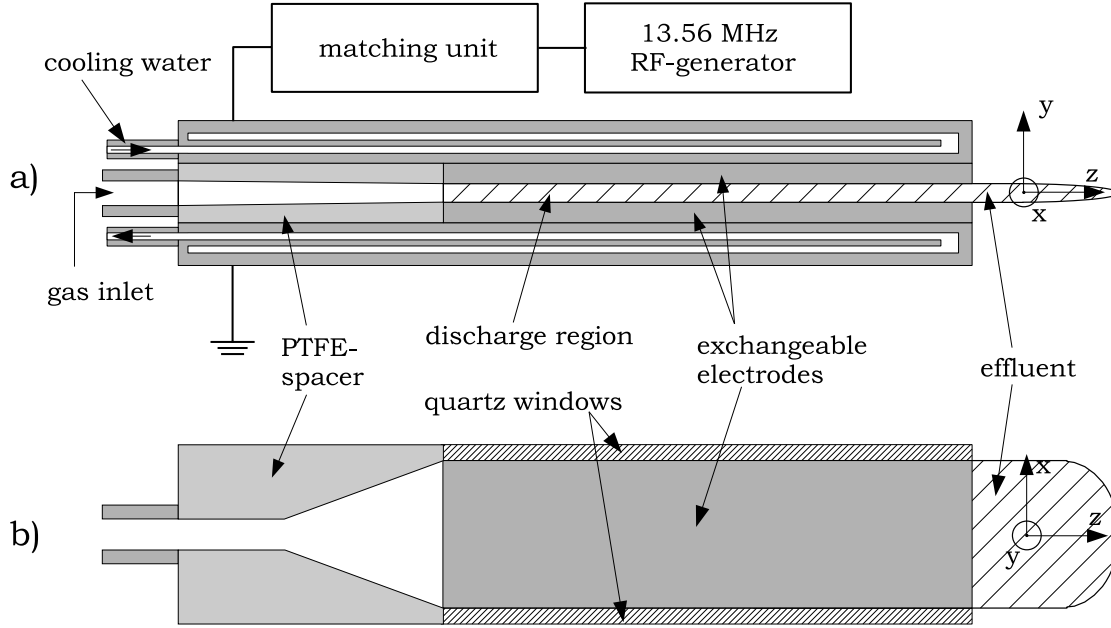
Figure 3.4: Sideview (a) and topview (b) schematics of the planar APPJ

3.1.2 Planar APPJ

In this work, a new APPJ setup was developed. Since the classical concentric setup allows no full insight into the discharge region, the new jet is set up in a plane parallel version, so that a free line of sight through the plasma is now possible. Figure 3.4 shows a schematic of this planar APPJ. Width and cross sectional area of the electrode gap are the same as in the concentric setup, so that the operating conditions of planar and concentric jet are very much alike. In contrast to the classical APPJ setup, the planar APPJ, however, is constructed modular so that it can be operated with electrodes differing in material or thickness, which allows setups with varying electrode gap widths. Comparing measurements on the APPJ with gap widths of 1.1 mm and 2 mm respectively are described in chapter 6.1.1. The exchangeable electrodes are screwed to the upper and lower water cooled ($140 \, \mathrm{l\,h^{-1}}$) electrode mount. The upper electrode is connected to a 13.56 MHz RF-generator via an L-type matching unit, while the lower electrode is grounded. The high voltage electrode is additionally shielded by a grounded copper shielding, to reduce RF-interferences and to ensure a secure operation. The gas is fed in at the back of the jet through a PTFE-spacer. The cross section of the gas channel in the PTFE-spacer is largely kept constant, forming a transition from the circular profile of the gas conduct to the rectangular profile of the electrode gap. Apart from serving as a gas

supply, the spacer acts as an insulator between the 'hot' electrode and the grounded electrode. The electrode surfaces are electropolished. The sides of the jet are capped with glass (BK7) or quartz windows, to confine the gas flux. Operating the jet in arcing mode can damage the windows. Hence, the planar APPJ is constructed to allow a simple exchange of the windows. As defined in figure 3.4 and used throughout this work, the x-axis denotes the axis perpendicular to the gas flow and parallel to the discharge gap, the y-axis is perpendicular to the gas flow and perpendicular to the discharge gap, and the z-axis is in direction of the gas-flow.

3.2 Working Principle of the APPJ

The APPJ shows a distinct non-thermal behaviour: It has a very low gas temperature ($< 100\,°C$) and physical model calculations [Park00] estimate an electron temperature of 2 to $4\,eV$. The electron density is approximately 0.2 to $2 \cdot 10^{11}\,cm^{-3}$ [ibid.]. As already mentioned in chapter 1.3, stabilisation of a glow discharge at atmospheric pressure is by no means trivial. The APPJ's glow discharge stability is established by the following mechanisms: First of all, there is the stabilising effect of radio frequency by ion trapping [Roth07]. Secondly, arcing is prevented by the use of helium as main feed gas which limits ionisation, and by the use of high gas flow rates which reduce the conductivity of the plasma [Raizer01]. Thirdly, active cooling of the electrodes (enhanced by a high gas flux) keeps the gas temperature constant and prevents thermal instability of the glow discharge. A special design of the electrodes is listed as a further stabilisation mechanism in the APPJ patent by Selwyn et al. [Selwyn99]. The stabilising principle is described as follows: There is evidence that indicates that electron density required for plasma sustenance is increased by minimising electron losses by electron trapping by means of the hollow cathode effect; that is, by sheath repulsion at all surfaces along the cavity, except in the axial flow direction [Selwyn99]. This design, however, is only of minor importance for a stable glow discharge mode. It is omitted in the layout of the APPJ used in this study.

Previous works by the AG Döbele[1] proved that the APPJ can be operated in argon [Wang03], although the higher breakdown voltage may cause a rapid multiplication of electrons after breakdown and lead to the formation of streamers or of a filamentary arc [Park01].

---

[1]Institute of Laser and Plasma Physics, University of Essen (now Duisburg-Essen) − Prof. Dr. H. F. Döbele (www.ilp.physik.uni-essen.de/doebele).
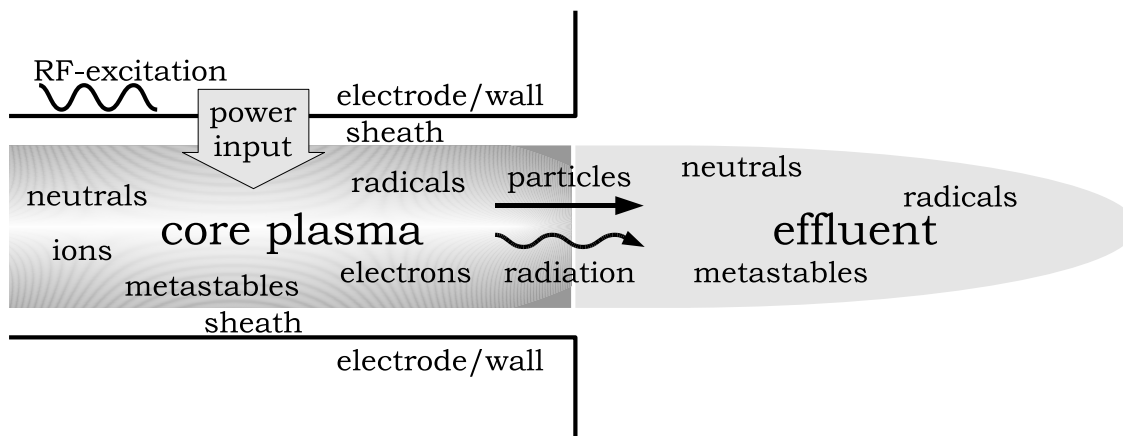
Figure 3.5:   Schematic of discharge region, effluent, and processes in the APPJ

3.2.1   Discharge Region and Effluent

Two substantial sections of the atmospheric pressure plasma jet need to be distinguished (see figure 3.5): The discharge region in between the electrodes consists of the core plasma in the centre and two plasma sheaths near the electrodes. Here the discharge is ignited and sustained by RF-power input. The plasma sheaths are regions where, due to their higher velocity only the electrons leave the plasma towards the electrodes, while the positive ions remain at their position. Thus, it is a positively charged region free of electrons. Due to the potential and charge distribution, the plasma sheaths represent capacitors [Raizer95]. Their thickness lies in the order of a few hundred µm [Shi05]. The discharge contains neutrals, radicals, metastables, electrons and ions, and radiation. The species can interact with the electrode walls.

The second substantial region is the effluent, leaving the jet through the nozzle. Here the particle distribution differs significantly from the discharge region. Already at a distance of a tenth of a millimetre, at a flow rate of $12.5 \, \mathrm{ms^{-1}}$, one can neglect the influence of the charged species on the reaction chemistry: The recombination coefficient for ions and electrons at atmospheric pressure is approximately $10^{-6} \, \mathrm{cm^3 s^{-1}}$, yielding a charged particle density of only $10^{11} \, \mathrm{cm^{-3}}$ after $10 \, \mathrm{\mu s}$ [Jeong00]. This value is well below the concentrations of the reactive neutral species, which are in the range of $10^{15} \, \mathrm{cm^{-3}}$ (see chapter 4). Species expected to be present in the effluent are therefore neutrals, oxygen radicals, and metastables. Also the radiation in the effluent needs to be considered. Discharge and effluent will be characterised in the following.